

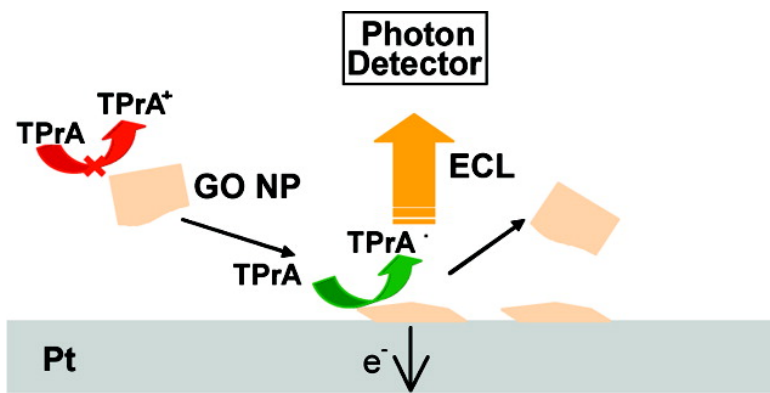
Communication

## Electrogenerated Chemiluminescence of Partially Oxidized Highly Oriented Pyrolytic Graphite Surfaces and of Graphene Oxide Nanoparticles

Fu-Ren F. Fan, Sungjin Park, Yanwu Zhu, Rodney S. Ruoff, and Allen J. Bard

*J. Am. Chem. Soc.*, 2009, 131 (3), 937-939 • DOI: 10.1021/ja8086246 • Publication Date (Web): 31 December 2008

Downloaded from <http://pubs.acs.org> on April 6, 2009



### More About This Article

Additional resources and features associated with this article are available within the HTML version:

- Supporting Information
- Access to high resolution figures
- Links to articles and content related to this article
- Copyright permission to reproduce figures and/or text from this article

[View the Full Text HTML](#)



**ACS Publications**

High quality. High impact.

Journal of the American Chemical Society is published by the American Chemical Society. 1155 Sixteenth Street N.W., Washington, DC 20036

# Electrogenerated Chemiluminescence of Partially Oxidized Highly Oriented Pyrolytic Graphite Surfaces and of Graphene Oxide Nanoparticles

Fu-Ren F. Fan,<sup>\*†</sup> Sungjin Park,<sup>‡</sup> Yanwu Zhu,<sup>‡</sup> Rodney S. Ruoff,<sup>‡</sup> and Allen J. Bard<sup>\*†</sup>

*Center for Electrochemistry, Department of Chemistry and Biochemistry and the Department of Mechanical Engineering, the University of Texas at Austin, Austin, Texas 78712*

Received November 7, 2008; E-mail: ajbard@mail.utexas.edu

We report here fairly intense electrogenerated chemiluminescence (ECL) from electrochemically oxidized highly oriented pyrolytic graphite (HOPG) and from a suspension of graphene oxide platelets. Low-dimensional nanostructures (nanotubes, nanobelts, nanowires, nanorods, and nanosheets) of a variety of materials have been actively studied because of their distinctive geometries, novel physical and chemical properties, and potential applications, for example, in nanoscale optical, mechanical, and electrical devices. For example, graphene, a one-atom thick sheet of carbon, and its oxidized form, graphene oxide, are of interest for their novel properties and potential applications.<sup>1–4</sup> Pristine graphene exhibits a strong ambipolar electric field effect,<sup>5</sup> quantum confinement, and quantum Hall effect,<sup>6</sup> while typically graphene oxide is insulating, depending on the coverage by epoxide and hydroxyl groups.<sup>7</sup> The mechanical properties of these intrinsically stiff materials have been investigated in some degree, but their luminescence properties still have not been studied and reported in detail. ECL<sup>8</sup> intensity of  $>4 \times 10^8$  photon counts  $s^{-1} cm^{-2}$  was found with oxidized HOPG and of  $>1.8 \times 10^6$  photon counts  $s^{-1} cm^{-2}$  from a 6 ppm suspension of graphene oxide platelets in an aqueous solution containing 0.1 M NaClO<sub>4</sub>, PBS (pH = 7.0) and 13 mM tri-*n*-propylamine (TPrA).

TPrA is widely used as a coreactant in ECL studies, because it generates a strongly reducing radical species upon oxidation.<sup>8</sup> Even in the absence of a luminescent species, oxidation of TPrA at an “inert” electrode, like Pt, Au, or glassy carbon (GC), is known to produce a very weak emission of light.<sup>9</sup> However, electrochemical and ECL studies show that an electrochemically oxidized HOPG electrode (area  $\approx 0.07 cm^2$ ) produces a quite strong emission. As shown in Figure 1 panels A and B, the ECL starts at the same potential where appreciable anodic faradaic current begins to flow. The cyclic voltammogram (CV) in the presence of TPrA shows a rather broad irreversible anodic wave starting at  $\sim 0.80$  V and peaking at  $\sim 1.35$  V vs SCE owing to the direct oxidation of TPrA; the shape of the corresponding ECL with potential is similar. This emission on HOPG is orders of magnitude higher than emission seen with Pt or GC. Figure 1D shows the ECL spectrum from a HOPG electrode in the presence of 13 mM TPrA.<sup>10</sup> The ECL spectrum extended from the near-infrared (NIR) to the green with three distinct maxima near 750, 670, and 610 nm and probably a shoulder near 570 nm, suggesting that emission might come from different emitting centers on the oxidized HOPG. The corresponding photoluminescence (PL) spectra at two different excitation wavelengths ( $\lambda_{ex} = 430$  and 440 nm) are shown in Figure 1C. They show a strong emission peak near 725 nm and a smaller, fairly broad emission from 525 to 700 nm, which are superimposed with several very sharp peaks probably due to scattering (for example, Raman scattering), since their positions shift nearly the same amount

as the difference in the excitation wavelengths. The ECL peak near 750 nm is apparently broader and red-shifted as compared to the sharp PL peak near 725 nm. However, considering the coarse wavelength interval, 25 nm, of the band-pass filters used in the ECL measurement, the ECL and PL peaks probably show similar wavelength peaks ( $750 \pm 25$  nm) in this wavelength region and thus the excited-state luminophores of these ECL and PL peaks are basically the same. Since a pure graphite crystal with low defect density does not photoluminesce in the visible region, the emitting centers must involve other sites on the electrode surface. Since carbon electrodes are known to oxidize and form oxygen-containing species upon anodization in aqueous solutions,<sup>11</sup> such sites are reasonable candidates.

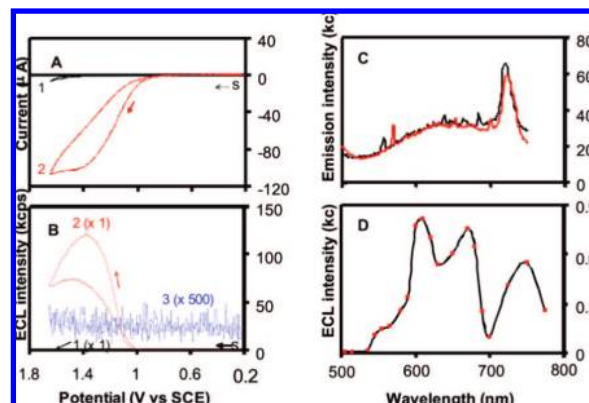


**Figure 1.** CV (A) and ECL intensity vs potential (B): (black) 0.1 M NaClO<sub>4</sub> and PBS only; (red) with addition of 13 mM TPrA; (blue) expanded scale of ECL intensity of curve 1. Potential scan rate = 20 mV/s at an HOPG electrode (area =  $0.07 cm^2$ ). (C) Photoluminescence in air of an HOPG electrode after ECL experiments. Excitation wavelength is 430 nm (black) and 440 nm (red). (D) ECL spectrum of HOPG in 0.1 M NaClO<sub>4</sub>, PBS (pH 7.0) containing 13 mM TPrA. Filter bandwidth = 5–10 nm in the range of wavelength studied, and data acquisition interval = 5–10 nm in the range of 500–700 nm but 25 nm beyond 700 nm. The red squares are the data and the black curve is “a guide to the eye”.

One approach to studying whether graphitic oxides luminesce and produce ECL, is to examine dispersions of graphite oxide (GO), which consist of primarily monolayer flakes, thus referred to here as ‘graphene oxide’ nanoparticles (NPs). Graphite oxide was synthesized from natural graphite (SP-1, Bay Carbon, MI) by a modified Hummers method.<sup>12</sup> A more detailed description about the preparation procedure of the suspension of graphene oxide NPs and its UV-vis-NIR absorbance is given in the Supporting Information. The resulting stock colloidal solution (3 mg GO in 10 mL of mixed solvent (water:ethanol = 1:9 by volume)) is a transparent brownish solution that exhibits weak light scattering. A typical SEM image of the graphene oxide NPs is shown in Figure

<sup>†</sup> Center for Electrochemistry, Department of Chemistry and Biochemistry.  
<sup>‡</sup> Department of Mechanical Engineering.

2, which shows that their lateral dimension ranges from  $\sim 100$  nm to  $\sim 1 \mu\text{m}$  and AFM images<sup>2</sup> revealed the presence of sheets with uniform thickness of  $\sim 1$  nm. More detailed imaging information is shown in the Supporting Information. An aliquot of 1–40  $\mu\text{L}$  of this solution was injected into about 2 mL of test electrolyte in the electrochemical cell yielding a particle concentration in the test solution in the range of 150 ppb to 6 ppm (12  $\mu\text{g}$  of GO in 2 mL of water or an average of  $9 \times 10^{10}$  graphene oxide NPs per mL of the test solution, see the discussion in the Supporting Information after the solutions are mixed).

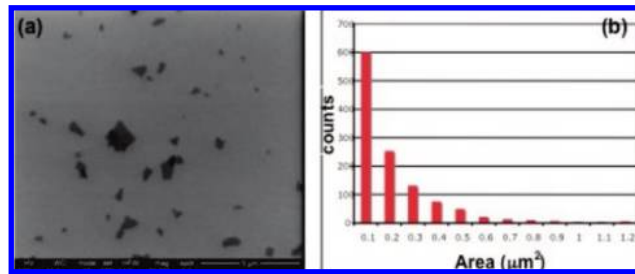


**Figure 2.** (a) A typical SEM image of graphene oxide sheets on a polished Si substrate; (b) a statistical distribution of the size based on the measurement of 1188 graphene oxide sheets.

Figure 3 (black curves) shows the UV–visible–NIR absorption spectrum of a suspension of graphene oxide NPs, which is similar to that reported previously.<sup>13</sup> An absorbance starts at about 800 nm (1.5 eV) and gradually increases at shorter wavelengths. The shape of the absorption spectrum and the vanishing of the extrapolated absorbance at low energy is consistent with a semiconductor with a distribution of highest occupied molecular orbital–lowest unoccupied molecular orbital (HOMO – LUMO) gaps or an indirect energy gap.<sup>14</sup> Considering that the spectrum is an average over graphene oxide NPs of different sizes<sup>2</sup> with different domain sizes of polycyclic aromatic hydrocarbon (PAH)<sup>15</sup> moieties or different chemical compositions<sup>7</sup> in the suspension, a distribution of energy gaps is not unexpected. The absorbance of a suspension<sup>16</sup> of partially reduced graphene oxide NPs extends to much longer wavelengths, indicating that such NPs have much smaller apparent energy gaps than the unreduced graphene oxide NPs.

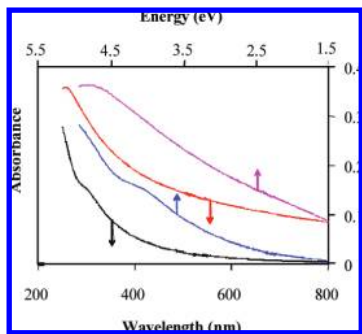
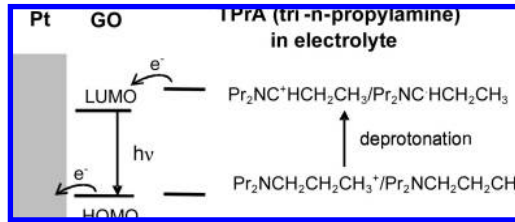


**Figure 3.** UV–vis–NIR spectra of graphene oxide (black and blue curves) and a partially reduced graphene oxide suspension (red and pink curves). Concentration of graphene oxide or the partially reduced graphene oxide, 6 ppm. Bottom scale, absorbance vs wavelength; top scale, absorbance vs energy.

To study ECL of individual graphene oxide NPs, we adopted a recently developed method for observing the collisions of single NPs at an electrode through measurement of light emission produced by ECL.<sup>17</sup> This technique is based on the significant

intensity amplification and fast temporal response of ECL involved in a rapid electrochemical reaction of a species and its coreactant in single particle collision events. The reactions of the species and the coreactant at relatively high concentrations of coreactant in solution can generate an appreciable ECL intensity at a conductive measuring electrode (Pt) at a given potential (Scheme 1). As shown in the black curve of Figure 4B, at a platinum electrode (area  $\sim 0.07 \text{ cm}^2$ ) immersed in a 0.1 M NaClO<sub>4</sub> solution containing phosphate buffer (pH 7.0) only, no appreciable ECL intensity was observed in the potential range studied (0.20–1.65 V vs SCE), although

#### Scheme 1



significant background oxidation current was observed at potentials positive of  $\sim 1.15$  V (black curve of Figure 4A). When both graphene oxide NPs and a coreactant (e.g., 13 mM TPrA) are present, a significant enhancement in the ECL signal intensity can be observed at potentials positive of 1.15 V (blue curve of Figure 4B), whereas only a small amount of ECL is detected in the presence of TPrA alone (see red curve of Figure 4B). Under similar conditions (similar concentrations of NPs and coreactant, supporting electrolyte and PBS, and same range of potential), a suspension of partially reduced graphene oxide NPs produced only weak ECL enhancement, perhaps because it forms a visible precipitate (not shown). The CV in the presence of TPrA (Figure 4A) shows a rather broad irreversible anodic wave due to the direct oxidation of TPrA. Note that the presence of graphene oxide NPs in the concentration range studied had essentially no effect on the CV. The oxidation current starts to rise at  $\sim 0.80$  V. This completely irreversible anodic oxidation behavior is similar to that of TPrA in neutral aqueous solution at a glassy carbon electrode.<sup>18</sup> The current and ECL intensity transients at a Pt electrode in a solution before and after injecting graphene oxide NPs are shown in Figure 4C,D.

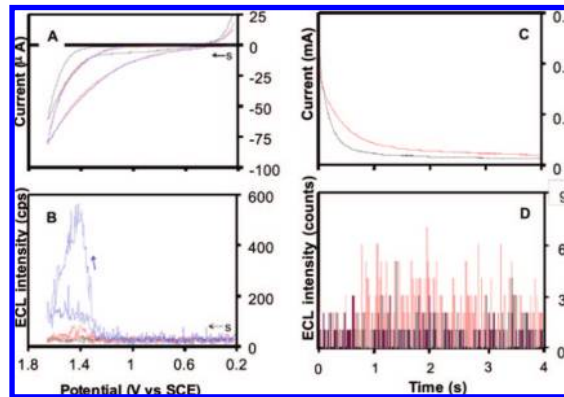


**Figure 4.** Current and ECL emission of graphene oxide: (A) CV, (B) ECL intensity vs potential. (Black) 0.1 M NaClO<sub>4</sub> and PBS only; (red) additional 13 mM TPrA; (blue) additional 6 ppm graphene oxide NP colloidal solution and 13 mM TPrA. The solution contained 0.1 M NaClO<sub>4</sub> as the supporting electrolyte and phosphate buffer (pH 7.0). Potential was stepped from 0.20 to 1.45 V vs SCE for 4 s (channel dwell time,  $\tau_{ch} = 15.6$  ms). (C) Current transient. (D) ECL intensity vs time record before (black) and after (red) the addition of 6 ppm graphene oxide NP colloidal solution and 13 mM TPrA. The solution contained 0.1 M NaClO<sub>4</sub> as the supporting electrolyte and phosphate buffer (pH 7.0). Potential was stepped from 0.20 to 1.45 V vs SCE for 4 s (channel dwell time,  $\tau_{ch} = 15.6$  ms).

As observed previously,<sup>17</sup> in this set of experiments, one can clearly observe single ECL events. The current transients ( $i$  vs  $t$  curves) before and after injection of ~6 ppm graphene oxide solution showed a smooth decay in both cases, while the ECL transients ( $I$  vs  $t$  curves) are stochastic. More detailed descriptions about the transient behavior and data are given in the Supporting Information. Although the total ECL intensity from the graphene oxide suspension can be measured easily, we have not been able to obtain its ECL spectrum with a reasonable signal-to-noise ratio.

As shown in reaction Scheme 1, when the electrode potential is scanned to a value positive of ~1.15 V, further oxidation of graphene oxide NPs takes place either directly on the Pt electrode during collision or via TPrA radical cations. The deprotonation reaction of TPrA generates a highly reductive radical intermediate and the radiative recombination of this radical and the graphene oxide NP leads to the formation of the excited-state of graphene oxide for the generation of ECL. Note that an oxidized HOPG electrode shows a much stronger (~200 times) ECL intensity than that observed at a Pt electrode in a suspension of graphene oxide platelets, probably because the effective concentration (considering population and geometric factors) of the luminescent centers available for electron transfer is much higher with the HOPG surface.

To the best of our knowledge, this is the first report of ECL of graphite and graphene oxides. This can provide a useful approach to the study of the electrochemistry of carbon-based NPs other than metallic NPs such as Au or Pt, as well as the basis of highly sensitive electroanalytical methods. While most of the NP research has focused on the properties of ensembles,<sup>19</sup> exploration at the single NP level is also of interest.<sup>17,20</sup> Further studies are underway to elucidate the ECL mechanism of graphene-based nanomaterials.

In summary, ECL emission is obtained from both a prepared suspension of graphene oxide NPs and an electrochemically oxidized graphite layer on HOPG. The nature of the emitting centers is under investigation, but a possible explanation of the broad emission is the existence of smaller aromatic hydrocarbon-like domains<sup>15</sup> formed on the “graphitic” layers by interruption of the conjugation by oxidized centers. ECL of individual graphene oxide NPs was detected by using a coreactant at relatively high concentration. With appropriate surface derivatization and functionalization<sup>11,21</sup> on graphene or graphene oxide to enhance the ECL efficiency and the accessibility to the substrate, highly sensitive analytical applications may emerge.

**Acknowledgment.** The support of this research by The UT Center for Electrochemistry and the Robert A. Welch Foundation and the assistance of M. Shen are gratefully acknowledged. S.J.P., Yanwu Zhu, and R.S.R. are supported by University of Texas startup funds.

**Supporting Information Available:** Detailed procedures for the syntheses of graphite oxide, preparation of graphene oxide and of partially reduced graphene oxide suspensions and procedures to prepare and characterize relatively pure graphene oxide of one-atom thickness (nanosheets) from natural graphite, and additional ECL and microscopy characterization results. This material is available free of charge via the Internet at <http://pubs.acs.org>.

## References

- (1) Geim, A. K.; Kim, P. K. *Sci. Am.* **2008**, 298, 90–97.
- (2) Stankovich, S.; Dikin, D. A.; Piner, R. D.; Kohlhaas, K. A.; Kleinhammes, A.; Jia, Y.; Wu, Y.; Nguyen, S. T.; Ruoff, R. S. *Carbon* **2007**, 45, 1558–1565.
- (3) Dikin, D. A.; Zimney, E. J.; Stankovich, S.; Piner, R. D.; Dommett, G. H. B.; Evmenenko, G.; Nguyen, S. T.; Ruoff, R. S. *Nature* **2007**, 448, 457–460.
- (4) Hernandez, Y.; Nicolosi, V.; Lotya, M.; Blighe, F. M.; Sun, Z.; De, S.; McGovern, I. T.; Holland, B.; Byrne, M.; Gun'ko, Y. K.; Boland, J. J.; Niraj, P.; Duesberg, G.; Krishnamurthy, S.; Goodhue, R.; Hutchison, J.; Scardaci, V.; Ferrari, A. C.; Coleman, J. N. *Nanotechnol.* **2008**, 3, 563–568.
- (5) Novoselov, K. S.; Geim, A. K.; Morozov, S. V.; Jiang, D.; Zhang, Y.; Dubonos, S. V.; Grigorieva, I. V.; Firsov, A. A. *Science* **2004**, 306, 666–669.
- (6) (a) Novoselov, K. S.; Geim, A. K.; Morozov, S. V.; Jiang, D.; Katsnelson, M. I.; Grigorev, I. V.; Dubonos, S. V.; Firsov, A. A. *Nature* **2005**, 438, 197–200. (b) Zhang, Y.; Tan, Y.-W.; Stormer, H. L.; Kim, P. *Nature* **2005**, 438, 201–204. (c) Berger, C.; Song, Z.; Li, X.; Wu, X.; Brown, N.; Naud, C.; Mayou, D.; Li, T.; Hass, J.; Marchenkov, A. N.; Conrad, E. H.; First, P. N.; de Heer, W. A. *Science* **2006**, 312, 1191–1196.
- (7) Boukhvalov, D. W.; Katsnelson, M. I. *J. Am. Chem. Soc.* **2008**, 130, 10697–10701, and references cited therein.
- (8) Bard, A. J. Ed. *Electrogenerated Chemiluminescence*; Marcel Dekker: New York, 2004.
- (9) Zu, Y.; Bard, A. J. *Anal. Chem.* **2000**, 72, 3223.
- (10) The ECL spectrum was acquired by using a set of calibrated interference notch filters (bandwidth = 10 nm) coupled with an avalanche photodiode (APD)-based single photon counter (see ref 17). A similar ECL spectrum but with a considerably worse S/N ratio was also seen with a CCD camera (M. Shen, F.-R. F. Fan, and A. J. Bard, unpublished results).
- (11) McCreery, R. L. In *Electroanalytical Chemistry*; Bard, A. J., Ed.; Marcel Dekker: New York, 2007; Vol. 17, p 221.
- (12) Hummers, W.; Offeman, R. *J. Am. Chem. Soc.* **1958**, 80, 1339.
- (13) Li, D.; Müller, M. B.; Gilje, S.; Kaner, R. B.; Wallace, G. G. *Nanotechnol.* **2008**, 3, 101–105.
- (14) (a) Butler, M. A. *J. Appl. Phys.* **1977**, 48, 1914. (b) Earnest, J. J. In *Semiconductors and Semimetals*; Willardson, R. K.; Beer, A. C., Eds.; Academic Press: New York, 1967; Vol. 3, Chapter 6.
- (15) Müllen, K.; Rabe, J. P. *Acc. Chem. Res.* **2008**, 41, 511–520.
- (16) Partially reduced graphene oxide suspension was prepared by adding hydrazine to a basic graphene oxide suspension, stirring at 35 °C for 6 h and then diluting with water.
- (17) Fan, F.-R. F.; Bard, A. J. *Nano Lett.* **2008**, 8, 1746–1749.
- (18) Mann, C. K. *Anal. Chem.* **1964**, 36, 2424.
- (19) (a) Balakrishnan, K.; Datar, A.; Oitker, R.; Chen, H.; Zou, J.; Zang, L. *J. Am. Chem. Soc.* **2005**, 127, 10496. (b) Che, Y.; Datar, A.; Yang, X.; Nando, T.; Zhao, J.; Zang, L. *J. Am. Chem. Soc.* **2007**, 129, 6354.
- (20) (a) Sönnichsen, C.; Reinhard, B. M.; Liphardt, J.; Alivisatos, A. P. *Nat. Biotechnol.* **2005**, 23, 741–745. (b) Xiao, X.; Bard, A. J. *J. Am. Chem. Soc.* **2007**, 129, 9610. (c) Palacios, R. E.; Fan, F.-R. F.; Grey, J. K.; Suk, J.; Bard, A. J.; Barbara, P. F. *Nat. Mater.* **2007**, 6, 680–685. (d) Yu, J.; Fan, F.-R. F.; Pan, S.; Lynch, V. M.; Omer, K.; Bard, A. J. *J. Am. Chem. Soc.* **2008**, 130, 7196–7197. (e) Chang, Y.-L.; Palacios, R. E.; Fan, F.-R. F.; Bard, A. J.; Barbara, P. F. *J. Am. Chem. Soc.* **2008**, 130, 8906–8907.
- (21) (a) Wang, X.; Tabakman, S. M.; Dai, H. *J. Am. Chem. Soc.* **2008**, 130, 8152–8153. (b) Sun, X.; Liu, Z.; Welsher, K.; Robinson, J. T.; Goodwin, A.; Zaric, S.; Dai, H. *Nano Res.* **2008**, 1, 203–212.

JA8086246